Characterization of the South Atlantic Anomaly

Khairul Afifi Nasuddin[1], Mardina Abdullah[1,2], Nurul Shazana Abdul Hamid[3]

[1]Centre of Advanced Electronic and Communication Engineering, Universiti Kebangsaan Malaysia, Bangi, 43600, Malaysia
[2]Space Science Center (ANGKASA), Institute of Climate Change, Universiti Kebangsaan Malaysia, Bangi, 43600, Malaysia
5   [3]School of Applied Physics, Faculty of Science and Technology, Universiti Kebangsaan Malaysia, Bangi, 43600, Malaysia

Correspondence to: Nurul Shazana Abdul Hamid (zana@ukm.edu.my)

Abstract. This research intends to characterize the South Atlantic Anomaly (SAA) by applying power spectrum analysis approach. From the approach, the Hurst exponent can be determined. The motivation to study the SAA region is due to its

10   nature. A comparison was made between the stations in the SAA region and outside the SAA region during the geomagnetic storm occurrence (active period) and normal period where no geomagnetic storm occurred. The data for the occurrence of the active period was taken on 11 March 2011 while for normal period on 3 February 2011. The outcomes of the research revealed that the SAA region had a tendency to be persistent during active period and normal periods. It can be said, it experiences this characteristic because of the Earth's magnetic field strength. Through the research, it is found that as the Earth magnetic field

15   increases, it is likely to show an antipersistent value. This is found in the high latitude region. The lower the Earth magnetic field, the more it shows the persistent value as in the middle latitude region. In the region where the Earth magnetic field is very low like the SAA region it shows a tendency to be persistent.

1 Introduction

Electromagnetic radiation and charged particles from the Sun constantly reach the Earth (Domingos et al., 2017).

20   Protons and electrons from the aurora, the high-speed solar wind, the radiation belts, or large solar coronal mass ejections penetrate into the Earth's atmosphere in different regions of the terrestrial magnetosphere (Sinnhuber et al., 2016). On the other hand, the Earth is surrounded by an almost spherical magnetic field, the magnetosphere, and it is a natural shielding of the Earth's surface to solar and galactic cosmic-ray particles of up to several GeV in energy (Ugusto et al., 2016).

The Earth's magnetic field configuration determines the trapping and distribution of energetic ionized particles

25   (Badhwar, 1997). By far the most dominant of these fields is of core origin, accounting for over 97 per cent of the field observed at the Earth's surface and ranging in intensity from about 30 000 nT at the equator to about 50 000 nT at the poles (Sabaka et al., 2002). The interaction of the solar wind with the magnetic field and atmosphere of the Earth causes, among other effects, disturbances in the ionosphere (Andalsvik and Jacobsen, 2014). With the existence of the Earth's magnetic field, it protects the world from danger such as geomagnetic storm. But, there still exist a region where the Earth's magnetic field is the weakest;

known as the South Atlantic Anomaly (SAA). The region arises due to the offset of the Earth's dipole of about 436 km from the Earth's center towards direction of the southeast Asia (Asikainen and Mursula, 2008).

The SAA describes a low intensity magnetic field area which spans from east of Africa over the Atlantic Ocean to South America (Koch and Kuvshinov, 2015). Its extent area at the Earth's surface is continuously growing since the intensity

5   instrumental measurements are available covering part of the Southern Hemisphere and centered in South America (Pavón-Carrasco and De Santis, 2016). This region of weak magnetic field has expanded over time and also moved west-ward (Cnossen and Matzka, 2016). The existence of the SAA is linked closely with the geomagnetic field distribution (Heynderickx, 1996). From the high atmosphere and close outer space, SAA is seen as a sort of geomagnetic hole where electric and neutral particles can flow from the Van Allen belts and from the magnetosphere into the atmosphere below (Santis and Qamili, 2010).

10   In this region, the inner Van Allen radiation belt its nearest approach to the Earth's surface. This result a number of energetic particles in the SAA region larger compare to other places. The energetic particles captured by the geomagnetic field can reach to lower altitudes forming a high-radiation region (Zou et al., 2015).

The SAA plays a vital role for spacecraft orbiting in that region. Very few measurements have made in this region, in comparison to the other regions of the world (Federico et al., 2010). Therefore, this research aims to characterize the SAA

15   region based on the geomagnetic data collected from several observatories outside and inside this region.

This research focuses on characterizing the SAA by using power spectrum analysis method. This study was motivated by the nature of the SAA, in which the area over the SAA is described by an intense radiation near the Earth's surface because of the particularly weak local geomagnetic field. It appears as the preferred way-in for high-energy particles in the magnetosphere, alongside the polar regions. As for satellite and spacecraft orbiting through the SAA, it will be beneficial to

20   have an update of the magnetic field strength as it can provide the regional magnetic intensity in that area.

1.1 Review of SAA and Power Spectrum Analysis

Space radiation is a very important factor affecting both humans and electronic systems (Konradi et al., 1994). The trapped radiation environment, consisting of large amounts of energetic charged particles, can be potentially harmful to human beings and space vehicles immerged in it (Qin et al., 2014). Geomagnetically trapped ionized particles, mainly electrons and

25   protons, are a hazard to modern spaceflight (Fürst et al., 2009). There are a number of damage spacecraft sustains whilst in orbit. These range from space debris, problems with the vacuum of space, various problems associated with the plasma environment, and various problems explicitly associated with the radiation environment (Heirtzler, 2002). One of the cases is with the International Space Station. It needs an additional shielding to deal with this sort of problem. Other examples are the Hubble Space Telescope that stops data collection whilst passing by the SAA. One SAA effect on the DORIS carrying satellites

30   is the shift of the onboard oscillator frequency (Capdeville et al., 2016). It is known that LEO (Low Earth Orbit) space vehicles spend a significant part of time in the SAA area (Grigoryan et al., 2008). Spacecraft in this area will receive the biggest radiation dose effect that is correlated by the intense fluxes of charged particles. Furthermore, astronaut's condition is influenced by the increased radiation in this area. Operators who control affected space vehicles need to know how best to

minimize the risk of anomalies which in many cases simply means knowing, with a high degree of accuracy, when and where to turn the systems on and off (Ginet et al., 2007).

Several researches has been conducted regarding SAA region. Study on the distribution of energetic particle fluxes near SAA, based on Kriging Interpolation, was conducted by Suparta et al. (2013). Kriging interpolation was used in this research to forecast the dissemination of solar charged particles in the SAA area. Data from electrons with 30 keV energy level (meped0e1) taken from the National Oceanic and Atmospheric Administration (NOAA) 15 satellite, on 8 September 2003 and 28 October in 2003 are employed (Suparta et al., 2013). The approach of Ordinary Kriging (OK) was selected since it is the finest linear unbiased estimator. Even so, this research also revealed a few dissymmetry of the estimate as well as variance figures meant for every model, particularly in the 0^0 longitude area. To resolve this difficulty, the robust variogram estimator usage was proposed.

Research on the radiation fields specific to the South Atlantic Anomaly was carried out by Panova et al. (1992). The research involves the explanation of the spatial as well as temporal behavior of the radiation field within the "MIR" space station through its passage of the South Atlantic Anomaly (SAA) region. The calculation of the radiation fields on the MIR station was carried out by means of the dosimeter "Lyulin". The measurements were carried out in the large diameter working compartment of the MIR station (Panova et al., 1992). The experiments was carry out to provide knowledge of the radiation fields precisely to the SAA as it bring valuable information for radiation safety on cosmonauts in the course of a long orbital flight.

One of the study on SAA is on the New Archeomagnetic Directional Records From Iron Age Southern Africa (ca. 425–1550 CE) and Implications for the South Atlantic Anomaly done by Hare et al. (2018). The new fine record comfirms the researchers earlier inferences that the SAA is the most current sign of a recurring event known as flux expulsion which has a serious effect on the manifestation of the Earth's magnetic field. Longer-term data from this region are crucial to understanding the current trend (Hare et al., 2018). In the research, a potential correlation of changes recorded in the African data accompanied by archaeomagnetism jerks were identify.

A research on the future of SAA in addition to implications for radiation harm in space was carried out by Heirtzler (2002). In this research, the SAA showed an important part in the radiation harm which happens close to the world's orbits. The significant plus current changes of the geomagnetic field in the South Atlantic was used in order to assess the size of the SAA up to the year 2000. This forecast pointed out that radiation harm towards spacecraft as well as mankind in space will very much rise plus current, covering a considerably greater geographical region than the present day. In general, this journal provides references for those who are interested in learning SAA.

The method chosen to characterize the SAA is called power spectrum analysis. Research on the spectral and fractal analyses of geomagnetic and riometric antarctic observations and a multidimensional activity index was done by Santis, Franceschi & Perrone (1997). Their study analyzed the geomagnetic and riometric data by using spectral and fractal analyses. A multidimensional index was obtained from this single-point data set to show the local and the global conditions of the magnetospheric activeness. Their work is a good reference of the power spectrum analysis.

Other studies include Fractal dynamics of geomagnetic storms done by Zaourar et al. (2013). In this work, the variations of the horizontal element of the Earth's magnetic field were studied. This was done to detect scaling reaction of the temporal changeability in geomagnetic data preserved by the Intermagnet observatories throughout the Solar Cycle 23. In this paper, the fractal spectral properties of the geomagnetic time series data were analyzed by applying spectral wavelet analysis

5   techniques.

Reseach on applying power spectrum analysis on the occurrence of sudden storm commencements (SSCs) for solar cycles 11 to 22 was done by Mendoza et al. (2003). The data for SSCs comprise solar cycles 11 to 22 (1868-1996) (Mendoza et al., 2003). The Maximum Entropy Method was opted to determine the power spectral density (PSD) of the SSCs time series, in addition to analyze their periodicities in the time series that were smoothed through obtaining a 13-month running mean.

10   The current research reveal the existence of a peak for the occurrence of SSCs between 20 to 30 y.

Jian-hui and Yao-quan (1995) apply power spectrum analysis for spherical volumes in order to investigate clustering of the Large Bright Quasar Sample. In order to avoid the effects of galactic absorption and foreground galaxies, most of the survey regions are located at galactic latitudes higher than 40^0 (Jian-hui and Yao-quan, 1995). The research was conducted to analyze the Large Bright Quasar Sample. In conclusion, the quasars of this sample is not clustered, or very weakly clustered.

15   Stations used in the study are situated within as well as outside the SAA area. Comparability will be made to describe the SAA through comparison of data from stations situated within the SAA area and station positions in the middle (mid) latitude area as well as high latitude region. This is done during the active period, which is the period of the geomagnetic storm occurrence and normal period where no geomagnetic storm occurred. The active period and normal period were chosen based on Kp Index and Dst Index.

20   Comprehensively, these make it an intriguing subject for characterizing the SAA. It can provide a better knowledge of the Earth-Space surrounding. Since a number of spacecrafts suffered hazards while orbiting through the SAA, it is hoped that this research can provide additional information about designing a better spacecraft to undergo the damage.

2 Methodology

2.1 Stations

25   Stations involved in the research were located inside and outside the SAA region. The list of the stations based on IAGA code, geodetic latitude and geodetic longitude can be seen in Table 1 while Fig. 1 shows their positions.

30

Table 1: Stations involved in the research.

SAA Region			
Station Name	IAGA CODE	Geodetic Latitude	Geodetic Longitude
Tsumeb	TSU	-19.202	17.584
Hermanus	HER	-34.425	19.225
Huancayo	HUA	-12.038	284.682
Ascension Island	ASC	-7.949	345.624
Vassouras	VSS	-22.400	316.400
Mid Latitude Region (Outside SAA Region)			
Station Name	IAGA CODE	Geodetic Latitude	Geodetic Longitude
Fresno	FRN	37.091	240.279
Fort Churchill	FCC	58.760	265.911
Newport	NEW	48.271	242.880
Sitka	SIT	57.061	224.669
Victoria	VIC	48.517	236.582
High Latitude Region (Outside SAA Region and Outside Mid Latitude Region)			
Station Name	IAGA CODE	Geodetic Latitude	Geodetic Longitude
College	CMO	64.871	212.139
Resolute Bay	RES	74.690	265.105
Baker Lake	BLC	64.319	263.988
Godhavn	GDH	69.250	306.470
Thule	THL	77.470	290.770

There are 15 stations involved, whereby five stations were located in the SAA region, five stations located in the mid latitude region and another five stations were at the high latitude region. The black circles in Fig. 1 show stations in the SAA 5 region while the magenta circles shows stations in the mid latitude region, and the blue circles represent stations in the high latitude region.
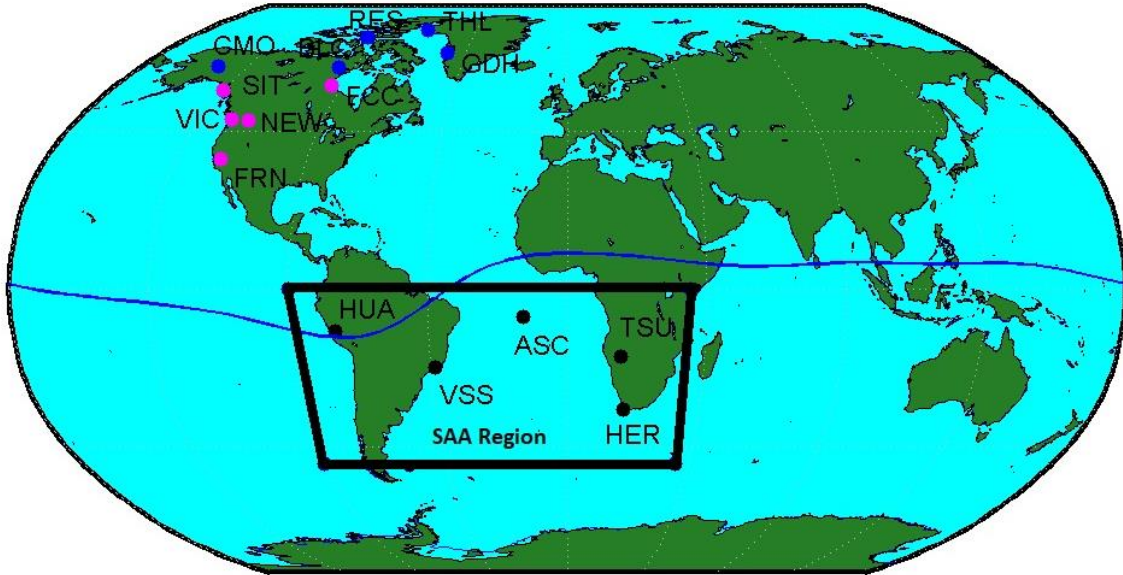
Figure 1: SAA is located at an altitude of 200-800 km above the earth's surface and extends from 0 to -50 degrees of latitude and from -90 to 40 degrees of longitude (Suparta et al., 2013). **The location of SAA region is based on Suparta et al. (2013). The black circle is the station in the SAA region.**

2.2 Power Spectrum Analysis and Hurst Exponent

The next step is to determine the power spectral density and its scaling with respect to frequency (Hall, 2014). The spectral analysis of a time series allows one to infer something regarding the characteristic time scales of the phenomena which give rise to the observed variations (Santis et al., 1997). A time series can be prescribed either in the time domain, as y_n, or in the frequency domain in terms of the discrete Fourier transform, Y_m (Malamud and Turcotte, 1999).

For power-spectral density function, which is represented as S_m, whereby it is intended for a discrete time series, represented by y_n, n = 1,2,3……..,N, can be inscribed as,

$$S_m = \lim_{N \to \infty} \{2\,|Y_m|^2/N\delta\}, \quad m = 1,2,3,\dots\dots,\frac{N}{2}, \tag{1}$$

It can also explain that δ is the time among consecutive n. In another situation, on behalf of a self-affine time series, the power-spectral density, represented as S_m, is described to comprise a power-law dependence on frequency

$$S_m \sim f_m^{-\beta}, \quad m = 1,2,3,\dots\dots,\frac{N}{2}, \tag{2}$$

It is to be denoted that $f_m = m/N$. It can also be explained that the value of β is an estimate of the intensity of persistence in a time series. For $-1 \le \beta < 1$, the Hurst exponent for a stationary fractional Gaussian noise time series is,

$$H_{PS} = (\beta + 1)/2 \,, \text{for} -1 \le \beta < 1 \,, \tag{3}$$

6

Nonlinear Processes
in Geophysics
Discussions

for a nonstationary fractional Brownian motion whereby the $1 < \beta \leq 3$ is represented by,

$$H_{PS} = (\beta - 1)/2 \, , \text{for } 1 < \beta \leq 3 \, , \tag{4}$$

It is important to understand the Hurst exponent, H, value. Time series with 0<H<0.5 are called antipersistent meanwhile time series with 0.5<H<1 are called persistent (Hamid et al., 2009).

5   If the Hurst exponent is in the range of 0.5-1, it reveals a time series with long-term positive autocorrelation, whereby it can be interpret as both that a high value in the series will probably be followed by another high value also that the values a long time into the future will serve to be high.

As for the Hurst exponent in the range of 0-0.5 means a time series with long-term switching between high and low values in adjacent pairs, indicating a single high value will may be succeeded by a low value and the following value will tend 10 to be high, with this trend to change between high and low values, continuing for a long time into the future.

2.3 Geomagnetic storm period and normal period

By using this method, a comparison between active period and normal period for the stations in the SAA region, mid latitude region, as well as high latitude region will be done. Active period can be define as a day from 1 UT until 24 UT where the existence of the geomagnetic storm is below – 30 nT. For normal period, it can be define as a day from 1 UT until 24 UT 15 whereby the value is consistently above -30 nT indicating no geomagnetic storm occurrence.

For this study, the date chosen for analysis was on 3 February 2011 for a normal period and on 11 March 2011 for an active period as shown in Table 2. Year 2011 was chosen to study the SAA during the rising phase of solar cycle 24.

Table 2: Date to be analyzed.

Active Period	Normal Period
11 March 2011	03 February 2011

20   The date for active period, 11 March 2011 was selected since during that day, the geomagnetic storm is consistently below -30 nT. Between 3 February 2011 and 11 March 2011, there are a number of geomagnetic storm occurrence. However, for the geomagnetic storm occurring on between those date, it can be seen the existing of the geomagnetic storm is inconsistent. For geomagnetic storm dates where it occurs consistently from 1 UT until 24 UT and closest to 3 February 2011, the date on which the geomagnetic storm occurred was on 11 March 2011. On that date, 11 March 2011, the geomagnetic storm was found 25 happens every time from 1 UT up to 24 UT according to Dst index.

The explanation on choosing 11 March 2011 compare to other date can be explain more detail by referring Fig. 2. It can be seen through the Dst index, for example, on 1 March 2011, despite geomagnetic storm events but it is inconsistent unlike the geomagnetic storm on 11 March 2011.
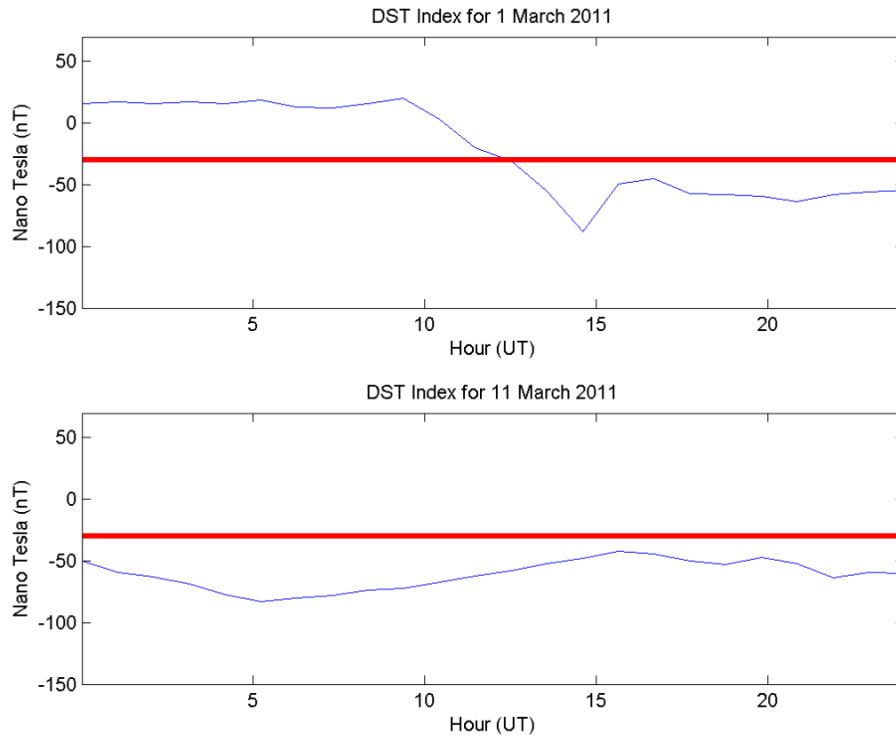
30

Figure 2: Comparison between geomagnetic storm on 1 March 2011 and 11 March 2011.

It is to be seen that on 1 March 2011, the geomagnetic storm started on that day at 13 UT up to 24 UT, but from 1 UT to 12 UT, no geomagnetic storm occurred. For the geomagnetic storm on 11 March 2011, it starts from 1 UT to 24 UT which is consistent throughout the day. The date of 11 March 2011 was also selected as it was closest to February 3, 2011.

2.4 Dst index and Kp index for geomagnetic storm period and normal period

Geomagnetic storm can be known through the Dst index and Kp index. It is to be noted that the red line in the Dst index is the threshold for a geomagnetic storm to occur. As the Dst Index is below -30 nT, it shows a geomagnetic storm occurrence . On 11 March in 2011, the Dst index shows a moderate storm, occurring from 1 to 14 UT, 18 to 19 UT and 21 to 24 UT. During 15 to 17 UT and on 20 UT a weak storm occurred. The Kp Index for the active period showed that on 11 March in 2011 a moderate geomagnetic storm occurred, with Kp Index showing at 6, and a minor geomagnetic storm occurred, with Kp Index showing at 5. Kp Index can be interpreted to show a geomagnetic storm had occurred when it has a value of 5 or larger than 5.
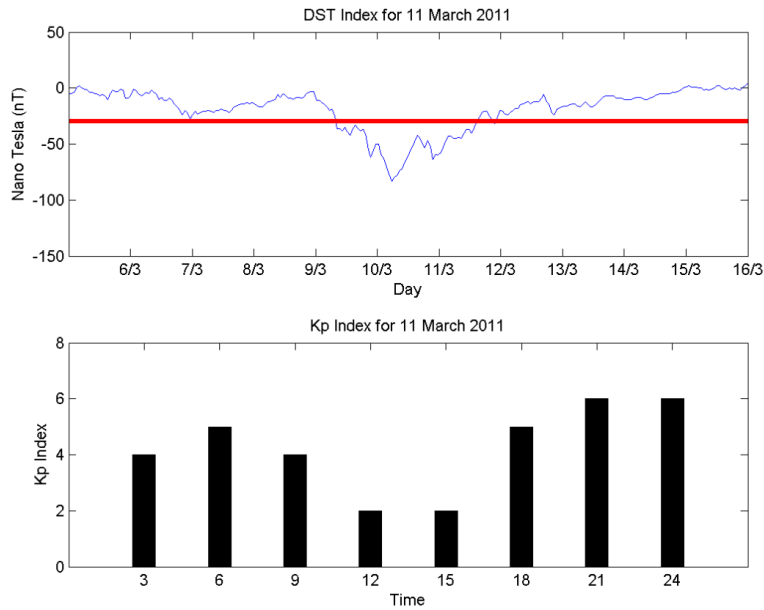
8

Figure 3: Dst Index and Kp Index for active period on 11 March 2011.

For the normal period, on 3 February in 2011, the Dst Index indicate no geomagnetic storm occurred. For the Kp Index, it shows mostly at 0 and 1 revealing no occurrence of geomagnetic storm.
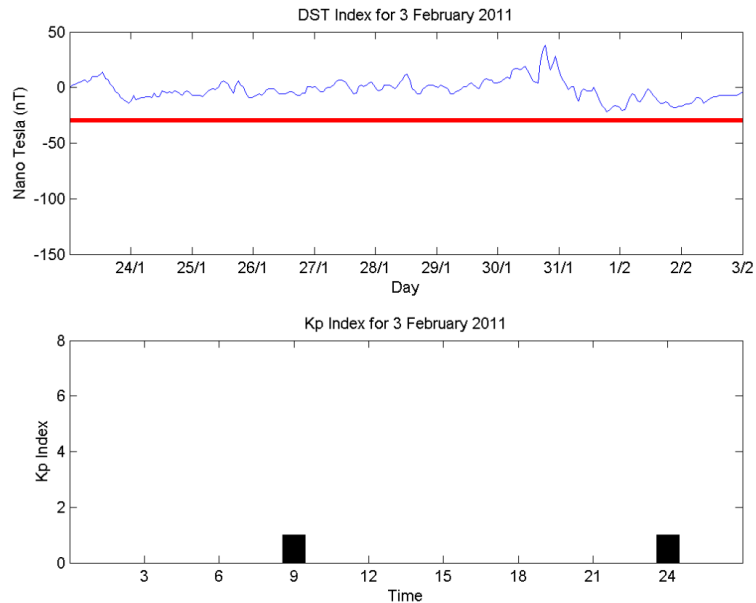
5

Figure 4: Dst Index and Kp Index for normal period on 3 February, 2011.

2.5 H-Component

The component of the Earth's magnetic field chosen to be analyzed is the horizontal intensity (H), since it is additionally sensitive towards geomagnetic activeness level. The sensitiveness of H can be described in Fig. 5. Figure 5 shows

5   the active time, whereby a geomagnetic storm occurred during that period. It can be shown that the beginning of a magnetic storm is frequently described by a global sudden rise in H, that is mentioned as the storm sudden commencement or moreover expressed as ssc. Subsequent to the ssc, the H component normally remains on top of its average level for several hours. This stage is named as the initial phase of the storm. Afterwards, a great global decrease in H commences, signifying the evolvement of the main phase of the storm. The amount of decrease in H describes the seriousness of disturbance. This can be shown in

10   Fig. 5.

Figure 5 shows the active time whereby the occurrence of geomagnetic storm happened in VSS station.
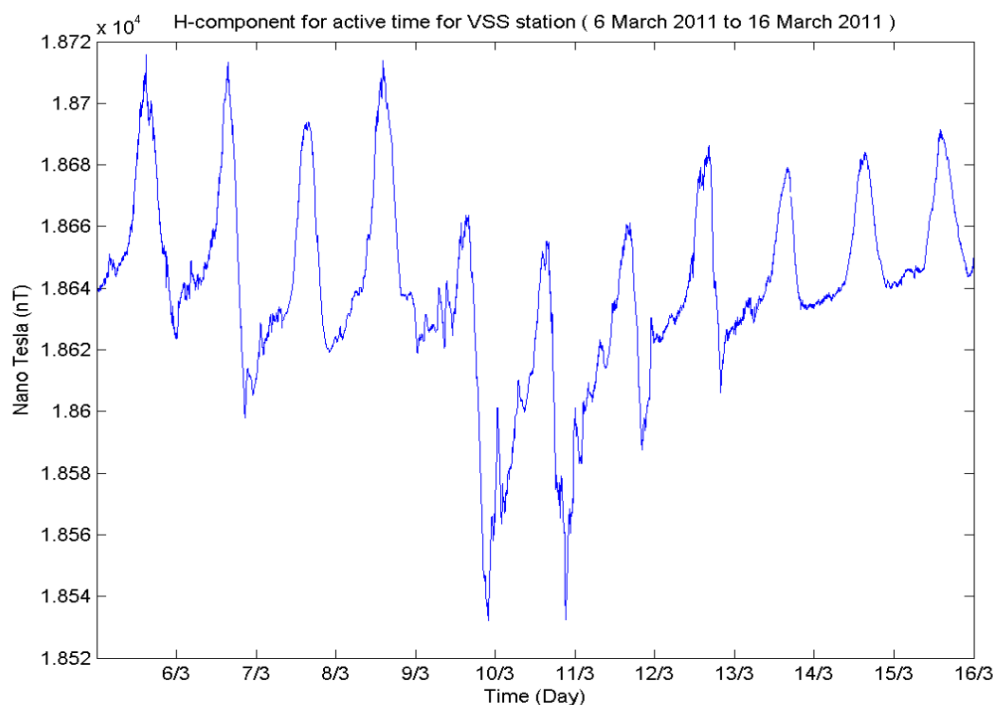

Figure 5: H-component during active time.

Nonlinear Processes
in Geophysics
Discussions

Open Access

EGU

3 Results and Discussion

Three regions were selected for this study; the first was high latitude region, second was mid latitude region, and third was the SAA region. A comparison between these regions was made to investigate the characteristics of the SAA region. Table 3, Table 4 and Table 5 show the research results. Table 3 shows the results for high latitude region during geomagnetic storm
5   period (active period) and normal period, while Table 4 presents the results for mid latitude region during geomagnetic storm (active period) and normal period. Table 5 represents the results of the SAA region. The maximum and minimum Earth's magnetic field strength for stations involved in the research are also shown in the tables during active and normal periods.

Table 3: Hurst exponent, the maximum and minimum Earth's magnetic field strength during geomagnetic storm
10   (active period) and normal periods for stations in high latitude region.

Station	Active Period			Normal Period		
	The Hurst exponent value	Minimum Earth magnetic field strength (nT)	Maximum Earth magnetic field strength (nT)	The Hurst exponent value	Minimum Earth magnetic field strength (nT)	Maximum Earth magnetic field strength (nT)
CMO	0.4116 ± 0.0601	56050	57060	0.1873 ± 0.0609	56910	56950
GDH	0.2840 ± 0.0379	56270	57160	0.1185 ± 0.0613	56500	56610
THL	0.5303 ± 0.0595	56360	56490	0.3915 ± 0.0629	56400	56410
RES	0.5936 ± 0.0669	57760	58010	0.2574 ± 0.0675	57820	57850
BLC	0.6466 ± 0.0878	58790	59440	0.0631 ± 0.0636	59090	59160

As for high latitude region, the stations chosen were from 60^0 to 90^0 latitude. It can be seen that the Hurst exponent value is varied. During active period, BLC, RES, THL stations showed persistent values with values of 0.6466 ± 0.0878, 0.5936 ± 0.0669 and 0.5303 ± 0.0595, respectively, while GDH and CMO stations showed antipersistent values of $0.2840 \pm$
15   0.0379 and 0.4116 ± 0.0601, respectively.

During the normal period, in the absence of a geomagnetic storm, the stations at high latitudes tend to record an antipersistent value. CMO, GDH, THL, RES and BLC stations values were 0.1873 ± 0.0609, 0.1185 ± 0.0613, 0.3915 ± 0.0629, 0.2574 ± 0.0675 and 0.0631 ± 0.0636, respectively. The obtained antipersistent values revealed a time series with

5   long-term switching between high and low values in adjacent pairs. It means a single high value may well be succeeded by a low value and the following value will tend to be high. This trend to alternate between high as well as low values will continue for a long time in the future.

It can be said the persistent and antipersistent experiences by stations in high latitude region may be associated with the strength of the Earth's magnetic field. The Earth's magnetic field value is strong in the high latitude area, thus providing a

10   high degree of antipersistent for stations in the high latitude region. Minimum and maximum Earth's magnetic field values in the active period range from 56050 nT to 58790 nT and 57060 nT to 59440 nT, respectively. During normal period, the minimum and maximum Earth's magnetic field ranges from 56910 nT to 59090 nT and 56950 nT to 59160 nT, respectively.

Table 4: Hurst exponent, the maximum and minimum Earth's magnetic field strength during geomagnetic storm
15   (active period) and normal period for station in mid latitude region.

Station	Active Period			Normal Period		
	The Hurst exponent value	Minimum Earth magnetic field strength (nT)	Maximum Earth magnetic field strength (nT)	The Hurst exponent value	Minimum Earth magnetic field strength (nT)	Maximum Earth magnetic field strength (nT)
FRN	0.6028 ± 0.0508	48760	48800	0.5779 ± 0.0683	48780	48810
VIC	0.6783 ± 0.0722	54200	54330	0.5352 ± 0.0624	54270	54280
NEW	0.6075 ± 0.0639	55170	55320	0.5342 ± 0.0632	55250	55260
SIT	0.3571 ± 0.0622	55750	56320	0.5055 ± 0.0680	56050	56070
FCC	0.3980 ± 0.0597	58410	59260	0.7066 ± 0.0561	58940	58980

Nonlinear Processes
in Geophysics
Discussions

Open Access

EGU

In the mid latitude regions, Earth's magnetic field values are not as strong as the high latitude region. The minimum and maximum values for the Earth's magnetic field during the active period were in the range of 48760 nT to 58410 nT and 48800 nT to 59260 nT, respectively. During normal periods, the minimum and maximum values of the Earth's magnetic field ranged from 48780 nT to 58940 nT and 48810 nT to 58980 nT, respectively. The Hurst exponent value showed a mixture of persistent and antipersistent values. SIT and FCC stations showed antipersistent values during active period. The value were 0.3571 ± 0.0622 and 0.3980 ± 0.0597. During normal period, the value was persistent with 0.5055 ± 0.0680 and 0.7066 ± 0.0561. As for VIC stations, NEW and FRN showed persistent values during active period and normal period.

It can be said that the value obtained in the mid latitude region differs from the value in the high latitude region during normal period and the active period may be due to different Earth's magnetic field values. Minimum Earth's magnetic field for mid latitude region during active period and normal period is from 48760 nT to 58410 nT and 48780 nT to 58940 nT, respectively. For the maximum Earth's magnetic field values were 48800 nT to 59260 nT during active period and 48810 nT to 58980 nT during normal period. This is in contrast to the high latitude region that has a higher Earth's magnetic field.

Table 5: Hurst exponent, the maximum and minimum Earth's magnetic field strength during geomagnetic storm (active period) and normal period for station in SAA latitude region.

Station	Active Period			Normal Period		
	The Hurst exponent value	Minimum Earth magnetic field strength (nT)	Maximum Earth magnetic field strength (nT)	The Hurst exponent value	Minimum Earth magnetic field strength (nT)	Maximum Earth magnetic field strength (nT)
VSS	0.6937 ± 0.0683	23270	23350	0.5259 ± 0.0537	23340	23360
HUA	0.5597 ± 0.0634	25210	25470	0.5434 ± 0.0692	25320	25410
HER	0.5871 ± 0.0613	25730	25820	0.5932 ± 0.0567	25760	25810
ASC	0.6232 ± 0.0519	28270	28350	0.5539 ± 0.0375	28350	28380
TSU	0.6002 ± 0.0569	29600	29650	0.6144 ± 0.0627	29640	29670

Nonlinear Processes
in Geophysics
Discussions

In the SAA region, the value was indicated as persistent during active period and normal period. VSS, HUA, HER, ASC and TSU stations during the active period it was indicated as persistent with values of 0.6937 ± 0.0683, 0.5597 ± 0.0634, 0.5871 ± 0.0613, 0.6232 ± 0.0519 and 0.6002 ± 0.0569, respectively. During normal periods, VSS, HUA, HER, ASC and TSU stations recorded persistent values with Hurst exponent at 0.5259 ± 0.0537, 0.5434 ± 0.0692, 0.5932 ± 0.0567, 0.5539 ± 0.0375 and 0.6144 ± 0.0627, respectively.

The minimum strength of Earth's magnetic field in SAA region during active period and normal period ranged from 23270 nT to 29600 nT and 23340 nT to 29640 nT, respectively. As for maximum Earth's magnetic fields in the active period and normal period, the values were 23350 nT to 29650 nT and 23360 nT to 29670 nT, respectively. It could be possible to say that the SAA region experienced this characteristic because of the weak Earth's magnetic field it exhibited whereby high energy particles in the SAA region effecting the value of the H-component.

4 Conclusion

From the research conducted, observation made shows that the persistent and antipersistent values experienced by stations in the high latitude region and mid latitude region and the persistent tendency the SAA region experienced during active period and normal period could be due to the influence of the strength of the Earth's magnetic field. Regions that have a strong Earth's magnetic field is more indicative to be anti persistent. This can be seen in the high latitude area. As the Earth's magnetic field decreases, the more likely it is to appear persistent. This is happening in low latitude region. Region where the Earth's magnetic field is very low, it shows a tendency for being persistent. This can be seen in the SAA region. The outcomes obtained from the research show that since the SAA region is persistent during active and normal periods in this study, it shows a time series with long-term positive autocorrelation, meaning that a high value in the series will probably be followed by another high value, and that the values for a long time into the future will to be high.

Data Availability

Data for this research can be obtained from INTERMAGNET. It can be accessed at www.intermagnet.org.

Author Contribution

Mardina Abdullah supervise the research and give approval as well as feedback. Nurul Shazana Abdul Hamid design the coding for power spectrum analysis and Hurst exponent and provide input on how the research should be done. Khairul Afifi Nasuddin do the research based on the supervision of Mardina Abdullah and Nurul Shazana Abdul Hamid and prepared the manuscript with contribution from all authors.

Nonlinear Processes in Geophysics
Discussions

Competing Interests

The authors declare that they have no conflict of interest.

Acknowledgements

References

Andalsvik, Y. L. and Jacobsen, K. S.: Observed high-latitude GNSS disturbances during a less-than-minor geomagnetic storm,
Radio Sci., 49, 1277–1288, doi:10.1002/2014RS005418, 2014.

10 Asikainen, T. and Mursula, K.: Energetic electron flux behavior at low L-shells and its relation to the South Atlantic Anomaly,
J. Atmos. Solar-Terrestrial Phys., 70, 532–538, doi:10.1016/j.jastp.2007.08.061, 2008.

Badhwar, G. D.: Drift rate of the South Atlantic Anomaly, J. Geophys. Res., 102, 2343–2349, doi:10.1029/96JA03494, 1997.

Capdeville, H., Petr, S., Hecker, L. and Lemoine, J.-M.: Update of the corrective model for Jason-1 DORIS data in relation to
the South Atlantic Anomaly and a corrective model for SPOT-5, Adv. Sp. Res., 58, 2628–2650, doi:10.1016/j.asr.2016.02.009,

15 2016.

Cnossen, I. and Matzka, J.: Changes in solar quiet magnetic variations since the Maunder Minimum: A comparison of historical
observations and model simulations, J. Geophys. Res. Sp. Phys., 121, 10520–10535, doi:10.1002/2016JA023211, 2016.

Domingos, J., Jault, D., Alexandra, M. and Mandea, M.: The South Atlantic Anomaly throughout the solar cycle, Earth Planet.
Sci. Lett., 473, 154–163, doi:10.1016/j.epsl.2017.06.004, 2017.

20 Federico, C. A., Gonçalez, O. L., Fonseca, E. S., Martin, I. M. and Caldas, L. V. E.: Neutron spectra measurements in the
south Atlantic anomaly region, Radiat. Meas., 45, 1526–1528, doi:10.1016/j.radmeas.2010.06.038, 2010.

Fürst, F., Wilms, J., Rothschild, R. E., Pottschmidt, K., Smith, D. M. and Lingenfelter, R.: Temporal variations of strength and
location of the South Atlantic Anomaly as measured by RXTE, Earth Planet. Sci. Lett., 281, 125–133,
doi:10.1016/j.epsl.2009.02.004, 2009.

25 Ginet, G. P., Madden, D., Dichter, B. K. and Brautigam G, D. H.: Energetic proton maps for the South Atlantic Anomaly, in:
IEEE Radiation Effects Data Workshop, Honolulu, HI, USA, 23-27 July 2007, 1–8, 2007.

Grigoryan, O. R., Romashova, V. V. and Petrov, a. N.: SAA drift: Experimental results, Adv. Sp. Res., 41, 76–80,
doi:10.1016/j.asr.2007.02.015, 2008.

Hall, C. M.: Complexity signatures in the geomagnetic H component recorded by the Tromsø magnetometer ($70 \circ N$, $19 \circ E$
30) over the last quarter of a century, Nonlin. Process. Geophys., 21, 1051–1058, doi:10.5194/npg-21-1051-2014, 2014.

Hamid, N. S. A., Gopir, G., Ismail, M., Misran, N., Hasbi, A. M., Usang, M. D. and Yumoto, K.: The Hurst exponents of the geomagnetic horizontal component during quiet and active periods, in: 2009 International Conference on Space Science and Communication, IconSpace - Proceedings, Negeri Sembilan, Malaysia, 26-27 Oct 2009, 186–190, 2009.

Hare, V. J., Tarduno, J. A., Huffman, T., Watkeys, M., Cottrell, R. D., Thebe, P. C., Manyanga, M. and Bono, R. K.: New

5 Archeomagnetic Directional Records From Iron Age Southern Africa (ca. 425–1550 CE) and Implications for the South Atlantic Anomaly, Geophys. Res. Lett., 45, 1361–1369, doi:10.1002/2017GL076007, 2018.

Heirtzler, J. R.: The future of the South Atlantic anomaly and implications for radiation damage in space, J. Atmos. Solar-Terrestrial Phys., 64, 1701–1708, doi:10.1016/S1364-6826(02)00120-7, 2002.

Heynderickx, D.: Comparison between methods to compensate for the secular motion of the South Atlantic Anomaly, Radiat.

10 Meas., 26, 369–373, doi:10.1016/1350-4487(96)00056-X, 1996.

Jian-hui, T. and Yao-quan, C.: Three dimensional power spectrum analysis of the Large Bright Quasar Sample, Chinese Astron. Astrophys., 19, 35–43, doi:10.1016/0275-1062(95)00007-F, 1995.

Koch, S. and Kuvshinov, A.: Does the South Atlantic Anomaly influence the ionospheric Sq current system? Inferences from analysis of ground-based magnetic data, Earth Planets Sp., 67, 1–7, doi:10.1186/s40623-014-0172-0, 2015.

15 Konradi, A., Badhwar, G. D. and Braby, L. A.: Recent space shuttle observations of the South Atlantic Anomaly and the radiation belt models, Adv. Sp. Res., 14, 911–921, doi:10.1016/0273-1177(94)90557-6, 1994.

Malamud, B. D. and Turcotte, D. L.: Self-affine time series: measures of weak and strong persistence, J. Stat. Plan. Inference, 80, 173–196, doi:10.1016/S0378-3758(98)00249-3, 1999.

Mendoza, B., Valdes-Galicia, J. F., Maravilla, D. and Lara, A.: Spectral analysis results for sudden storm commencements

20 1868–1996, Adv. Sp. Res., 31, 1075–1079, doi:10.1016/SO273-1177(02)00804-9, 2003.

Panova, N. A., Pftrov, V. M. and Shurshakov, V. A.: Radiation Fields Specific to the South Atlantic Anomaly, Nucl. Tracks Radiat. Meas., 20, 25–28, doi:10.1016/1359-0189(92)90080-F, 1992.

Pavón-Carrasco, F. J. and De Santis, A.: The South Atlantic Anomaly: The Key for a Possible Geomagnetic Reversal, Front. Earth Sci., 4, 1–9, doi:10.3389/feart.2016.00040, 2016.

25 Qin, M., Zhang, X., Ni, B., Song, H., Zou, H. and Sun, Y.: Solar cycle variations of trapped proton flux in the inner radiation belt, J. Geophys. Res. Sp. Phys., 119, 9658–9669, doi:10.1002/2014JA020300, 2014.

Sabaka, T. J., Olsen, N. and Langel, R. a.: A comprehensive model of the quiet-time, near-Earth magnetic field: phase 3, Geophys. J. Int., 151, 32–68, doi:10.1046/j.1365-246X.2002.01774.x, 2002.

Santis, A. De and Qamili, E.: Equivalent Monopole Source of the Geomagnetic South Atlantic Anomaly, Pure Appl. Geophys.,

30 167, 339–347, doi:10.1007/s00024-009-0020-5, 2010.

Santis, A. De, Franceschi, G. De and Perrone, L.: Spectral and fractal analyses of geomagnetic and riometric antarctic observations and a multidimensional index of activity, J. Atmos. Solar-Terrestrial Phys., 59, 1073–1085, doi:10.1016/S1364-6826(96)00084-3, 1997.

Sinnhuber, M., Friederich, F., Bender, S. and Burrows, J. P.: The response of mesospheric NO to geomagnetic forcing in 2002

Nonlinear Processes
in Geophysics
Discussions

Open Access

EGU

– 2012 as seen by SCIAMACHY, J. Geophys. Res. Sp. Phys., 121, 3603–3620, doi:10.1002/2015JA022284, 2016.

Suparta, W., Gusrizal, Mohd. Ali, M. A. and Ahmad, N.: Distribution of energetic particle fluxes in the vicinity of SAA according to Kriging interpolation, in: International Conference on Space Science and Communication, IconSpace, Melaka, Malaysia, 1-3 July 2013, 17–22., 2013.

5   Ugusto, C. A., Avia, C. N., Liveira, M. N. D. E. O. and Auth, A. F.: Signals at ground level of relativistic solar particles associated with a radiation storm on 2014 April 18, Publ. Astron. Soc. Japan, 68, 1–12, doi:10.1093/pasj/psv111, 2016.

Zou, H., Li, C., Zong, Q., Parks, G. K., Pu, Z., Chen, H., Xie, L. and Zhang, X.: Short-term variations of the inner radiation belt in the South Atlantic anomaly, J. Geophys. Res. Sp. Phys., 120, 4475–4486, doi:10.1002/2015JA021312, 2015.

10